

Fig. 5. Suppression effects of ICAM-1 siRNA delivery using Man-PEG₂₀₀₀ BLs and US exposure on liver toxicity in an LPS/D-galactosamine-induced inflammatory mouse model. (A) The level of serum ALT/AST activities following by siRNA delivery (10 μ g siRNA) using various methods at predetermined times after LPS/D-galactosamine stimulation. Each value represents the mean \pm SD (n=5). (B) Fluorescent images of apoptosis following by siRNA delivery using Man-PEG₂₀₀₀ BLs (10 μ g siRNA) and US exposure in LPS/D-galactosamine-stimulated mice. Apoptosis (green) was detected by TUNEL staining, and nuclei were counterstained with DAPI (blue). Scale bars, 100 μ m. (C) Liver histology with H&E staining at 24 h following siRNA delivery using Man-PEG₂₀₀₀ BLs (10 μ g siRNA) and US exposure in LPS/D-galactosamine-induced inflammatory mouse model. Black arrows: destruction of tube formation in hepatic central vein. Scale bars, 100 μ m.

119x118mm (600 x 600 DPI)

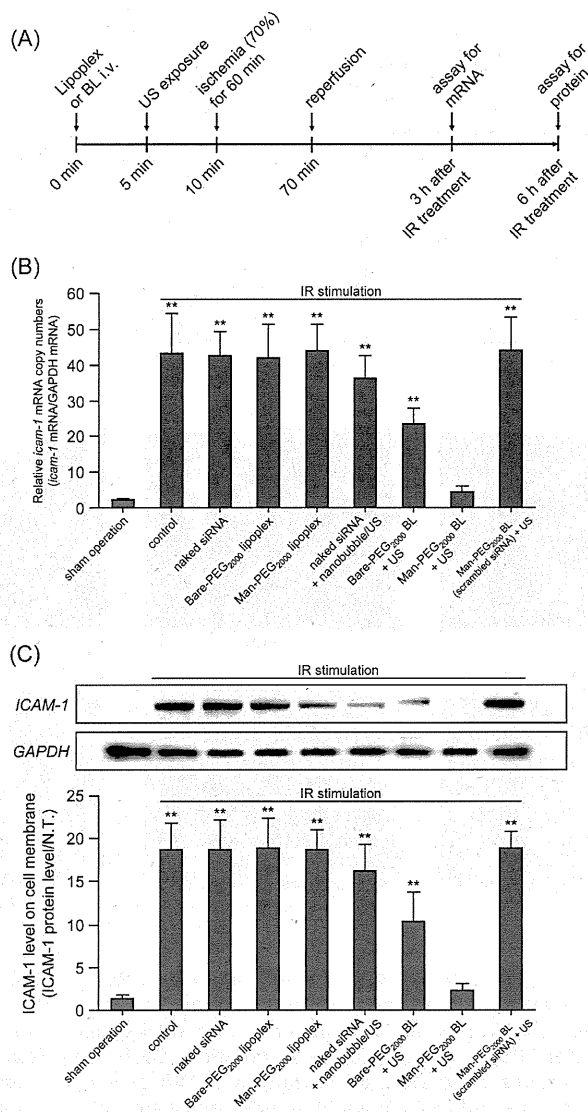


Fig. 6. Suppression effects of ICAM-1 siRNA delivery using Man-PEG₂₀₀₀ BLs and US exposure on *icam-1* mRNA and protein expression in HECs of an IR-induced hepatic inflammatory mouse model. (A) Evaluation schedule of ICAM-1 expression in hepatic IR-stimulated mice. (B, C) The expressing level of *icam-1* mRNA in the cells (B) and protein on the cell membrane (C) obtained by siRNA delivery (10 µg siRNA) using various delivery methods in HECs. HECs were isolated by collagenase perfusion, one-step density gradient centrifugation, and magnetic cell sorting according to *Supplementary Materials and Methods*. The *icam-1* mRNA and protein expression in HECs was determined by quantitative RT-PCR (B), western blotting/ELISA (C). The expression levels of mRNA and protein were detected at 3 and 6 h following IR-stimulation, respectively. * $P < 0.05$; ** $P < 0.01$, compared with sham operation. Each value represents the mean+SD (n=5). 148x275mm (600 x 600 DPI)

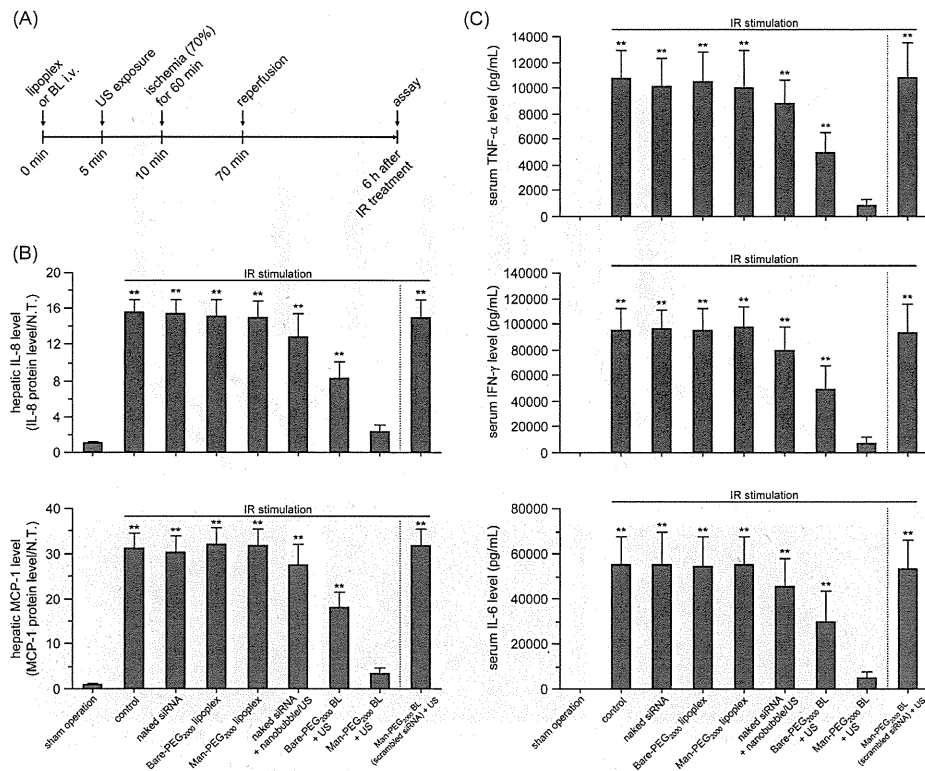


Fig. 7. Suppression effects of ICAM-1 siRNA delivery using Man-PEG₂₀₀₀ BLs and US exposure on leukocyte infiltration and pro-inflammatory cytokine production in IR-induced hepatic inflammatory mouse model. (A) Evaluation schedule of leukocyte infiltration and pro-inflammatory cytokine production in hepatic IR-stimulated mice. (B, C) The levels of IL-8, MCP-1 expression in the liver (B) and TNF- α , IFN- γ , IL-6 secretion in the serum (C) following by siRNA delivery (10 μ g siRNA) using various delivery methods at 6 h following IR-stimulation. ** $P < 0.01$, compared with sham operation. Each value represents the mean \pm SD (n=5).
116x96mm (600 x 600 DPI)

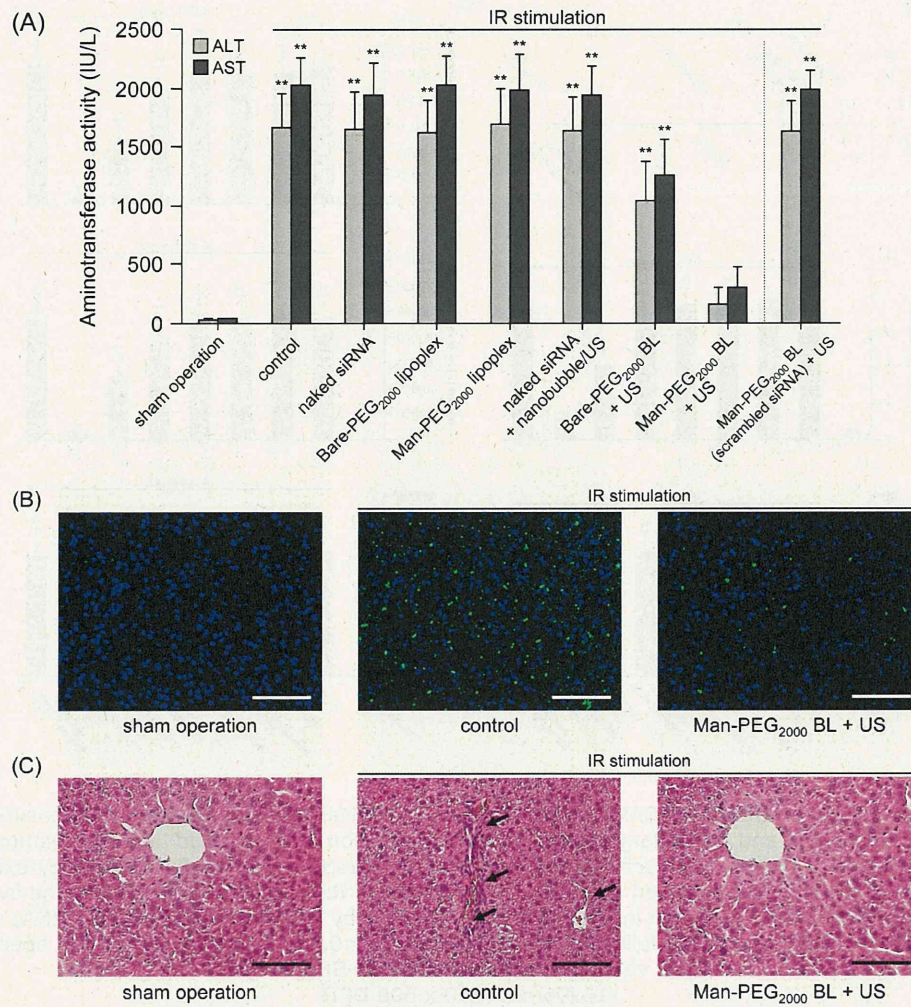


Fig. 8. Suppression effects of ICAM-1 siRNA delivery using Man-PEG₂₀₀₀ BLs and US exposure on liver toxicity in an IR-induced hepatic inflammatory mouse model. (A) The level of serum ALT/AST activities followed by siRNA delivery (10 μg siRNA) using various delivery methods at 24 h following hepatic IR-stimulation. ***P*<0.01, compared with the corresponding sham operation group. Each value represents the mean±SD (n=5). (B) Fluorescent images of apoptosis followed by siRNA delivery using Man-PEG₂₀₀₀ BLs (10 μg siRNA) and US exposure in IR-induced hepatic inflammatory mouse model. Apoptosis (green) was detected by TUNEL staining, and nuclei were counterstained with DAPI (blue). Scale bars, 100 μm. (C) Liver histology at 24 h following siRNA delivery using Man-PEG₂₀₀₀ BLs (10 μg siRNA) and US exposure in IR-induced hepatic inflammatory mouse model. Black arrows: destruction of tube formation in hepatic central vein. Scale bars, 100 μm. 131x143mm (600 x 600 DPI)

Hepatology

Original Research

Supplementary Information

Efficient suppression of murine ICAM-1 using ultrasound-responsive and mannose-modified lipoplexes inhibits acute hepatic inflammationKeita Un^{1,2}, Shigeru Kawakami^{1*}, Mitsuru Yoshida¹, Yuriko Higuchi³, Ryo Suzuki⁴, Kazuo Maruyama⁴, Fumiyoshi Yamashita¹, Mitsuru Hashida^{1,5*}

* corresponding authors

¹Department of Drug Delivery Research, Graduate School of Pharmaceutical Sciences, Kyoto University, 46-29 Yoshida-shimoadachi-cho, Sakyo-ku, Kyoto 606-8501, Japan.²The Japan Society for the Promotion of Science (JSPS), Chiyoda-ku, Tokyo 102-8471, Japan.³Institute for Innovative NanoBio Drug Discovery and Development, Graduate School of Pharmaceutical Sciences, Kyoto University, 46-29 Yoshida-shimoadachi-cho, Sakyo-ku, Kyoto 606-8501, Japan.⁴Department of Biopharmaceutics, School of Pharmaceutical Sciences, Teikyo University, 1091-1 Suwarashi, Sagamiko, Sagamihara, Kanagawa 229-0195, Japan.⁵Institute for Integrated Cell-Material Sciences (iCeMS), Kyoto University, Yoshida-ushinomiya-cho, Sakyo-ku, Kyoto 606-8302, Japan.

* corresponding authors

Mitsuru Hashida, Ph.D. and Shigeru Kawakami, Ph.D.

Department of Drug Delivery Research, Graduate School of Pharmaceutical Sciences, Kyoto University, 46-29 Yoshida-shimoadachi-cho, Sakyo-ku, Kyoto 606-8501, Japan.

Phone: +81-75-753-4545. Fax: +81-75-753-4575.

E-mail: hashidam@pharm.kyoto-u.ac.jp (M. Hashida)

kawakami@pharm.kyoto-u.ac.jp (S. Kawakami)

Supplementary Materials and Methods

siRNA and Mice. Individual siRNAs (21 mer) consisting of 3'-dTdT overhang sequences were chemically synthesized by GeneDesign (Osaka, Japan). The sequences of the synthesized siRNA are shown in Supplementary Figure 1A. As far as *in-vivo* experiments are concerned, the level of hepatic inflammatory responses induced by LPS-stimulation in female mice is higher than that in male mice [1]. Moreover, since our group has been used female mice in previous studies involved in inflammatory responses [2]; therefore, female mice were used in this study. Female C57BL6 mice (6-8 weeks old) were purchased from Japan SLC (Shizuoka, Japan). All animal experiments were performed in accordance with the Principles of Laboratory Animal Care as adopted and promulgated by the United States National Institutes of Health and the guidelines for animal experiments of Kyoto University, Japan.

Construction of Man-PEG₂₀₀₀ BLs. Synthesis of Man-PEG₂₀₀₀-DSPE and construction of Man-PEG₂₀₀₀ BLs were performed according to our previous report [3]. Briefly, 1,2-distearoyl-*sn*-glycero-3-trimethylammoniumpropane (DSTAP; Avanti Polar Lipids, Alabaster, AL), 1,2-distearoyl-*sn*-glycero-3-phosphocholine (DSPC; Sigma-Aldrich, St. Louis, MO) and 1,2-distearoyl-*sn*-glycero-3-phosphoethanolamine-N-[amino (polyethylene glycol)-2000] (NH₂-PEG₂₀₀₀-DSPE) or mannose-modified PEG₂₀₀₀-DSPE (NOF, Tokyo, Japan) were mixed in chloroform at a molar ratio of 7:2:1 to produce the liposomes for BLs. For construction of conventional nanobubbles [4], DSPC and methoxy-PEG₂₀₀₀-DSPE (NOF) were mixed in chloroform at a molar ratio of 94:6. For construction of liposomes, the mixture was dried by evaporation, vacuum desiccated and the resultant lipid film was resuspended in sterile 5% dextrose. After hydration for 30 min at 65 °C, the suspension was sonicated for 10 min in a bath sonicator and for 3 min in a tip sonicator to produce liposomes. Liposome suspensions were sterilized by passage through a 0.45 µm filter (Pall, East Hills, NY). The lipoplexes were prepared by gently mixing equal volumes of siRNA and liposome solution at a charge ratio of 1.0:2.3 (negative:positive). To enclose US imaging gas into lipoplexes, the prepared lipoplexes were pressurized with perfluoropropane gas (Takachiho Chemical Industries, Tokyo, Japan) and sonicated using a bath sonicator (A.S. One, Osaka, Japan) for 5 min. The particle sizes and ζ-potentials of the liposomes/lipoplexes were determined using a Zetasizer Nano ZS instrument (Malvern Instrument, Worcestershire, UK).

Separation of mouse PCs and NPCs. The isolation of mouse hepatic non-parenchymal cells (NPCs) was performed according to our previous reports [5]. Briefly, at 6 h after *in vivo* siRNA delivery using BLs and US exposure, each mouse was anesthetized with pentobarbital sodium (40-60 mg/kg) and the liver was perfused with perfusion buffer (Ca²⁺, Mg²⁺-free HEPES solution, pH 7.2) for 10 min. Then, the liver was perfused with collagenase buffer (HEPES solution, pH 7.5 containing 5 mM CaCl₂ and 0.05 % (w/v) collagenase (type I)) for 5 min. Immediately after the start of perfusion, the vena cava and aorta were cut and the perfusion rate was maintained at 5 mL/min. At the end of perfusion, the liver was excised. The cells were dispersed in ice-cold Hank's-HEPES buffer by gentle stirring and then filtered through cotton mesh sieves, followed by centrifugation at 50 × g for 1 min. The supernatant containing hepatic NPCs was similarly centrifuged 5 times and the resulting supernatant was centrifuged twice at 300 × g for 10 min. Then, the mouse HECs were isolated according to other reports [6,7]. Briefly, NPCs were separated from the supernatant by one-step density gradient centrifugation with 12.6% OptiPrep (Axis-Shield PoC AS, Oslo, Norway).

Isolation of mouse HECs. Mouse HECs abundantly express CD146 as a specific ligand. Therefore, to isolate mouse HECs, the separated mouse NPCs were mixed with anti-mouse CD146 antibody (ME-9F1)-conjugated microbeads (Miltenyi Biotec, Auburn, CA), and then, subjected magnetic cell sorting using auto MACS following the manufacturer's instructions. Isolated cells were seeded onto collagen-coated 24-well plates in DMEM supplemented with 10% FBS, 100 IU/mL penicillin, 100 µg/mL streptomycin, and 2 mM L-glutamine. Cells adhered within 24 h were washed and used as HECs after additional incubation for 72 h.

Cellular association study of siRNA. Lipoplexes and BLs were constructed with AlexaFluor-594 labeled ICAM-1 siRNA (GeneDesign), and ICAM-1 siRNA was transferred into HECs according to above-mentioned protocol. Endocytosis was inhibited by mannan (1 mg/mL) as inhibitor of mannose receptor, and chlorpromazine (50 µM) as clathrin-mediated endocytosis inhibitor. Each endocytosis inhibitor was added to cells at 30 min before the addition of lipoplexes. At 2 h after siRNA transfer, the cells were scraped from the plates and suspended in lysis buffer (0.05% Triton X-100, 2 mM EDTA, 0.1 M Tris, pH 7.8). Then, the cell suspension was shaken, and centrifuged at 10,000 × g, 4 °C for 10 min. Fluorescence intensity of the supernatant derived from AlexaFluoro-594 was measured with FluoroMax-4

(Horiba, Kyoto, Japan) and the fluorescence intensity was normalized with respect to the protein content of cells. The protein concentration was determined with a Protein Quantification Kit (Dojindo Molecular Technologies, Tokyo, Japan).

Confocal microscopy study. At 48 h incubation after HECs were collected, BLs constructed with AlexaFluor-594 labeled siRNA (GeneDesign) were added at a dose of 1 μ g siRNA. At 5 min after the addition of bubble lipoplexes, cells were exposed to US (frequency, 2.062 MHz; duty, 50%; burst rate, 10 Hz; intensity 4.0 W/cm²) for 20 s using a 6 mm diameter probe placed in the well. Endosomes were labeled with 100 μ g/mL AlexaFluor-488 transferrin conjugates (Invitrogen) before the addition of BLs. Cells were washed five times with ice-cold PBS, and fixed with 4% paraformaldehyde. Then, after washing twice with ice-cold PBS, cover glasses were mounted on slide glasses with VECTASHIELD mounting medium with DAPI (Vector Laboratories, Burlingame, CA). Samples were observed using a Fluoview FV10i confocal laser microscope (Olympus, Tokyo, Japan).

MTT assay. The cytotoxicity was evaluated by MTT assay. Briefly, at predetermined times following inflammatory stimulation, 3-(4,5-dimethyl-2-thiazol)-2,5-diphenyltetrazolium bromide (Nacalai Tesque, Kyoto, Japan) solution was added to each well and incubated for 4 h. The resultant formazan crystals were dissolved in 0.04 M HCl-isopropanol and sonicated for 10 min in a bath sonicator. Absorbance values at 550 nm (test wavelength) and 655 nm (reference wavelength) were measured and the results were expressed as viability (%).

Tissue distribution of radio-labeled lipoplexes. ICAM-1 siRNA complexes constructed with ³H-labeled liposomes ([³H]-DSPC; American Radiolabeled Chemicals, St. Louis, MO) were injected intravenously into mice. At predetermined times after administration, blood was collected from the vena cava under pentobarbital anesthesia. Then, mice were sacrificed and the organs were collected, rinsed with saline and weighed. The tissues were dissolved in Soluene-350 and the resultant lysates were decolorized with isopropanol and 30% H₂O₂, and then neutralized with 5 N HCl. The radioactivity of ³²P-labeled pDNA was measured in scintillation counter (LSA-500; Beckman Coulter, CA) after addition of Clear-Sol I solution.

Hepatic cellular localization of Alexa Fluoro-594 labeled siRNA. BLs constructed with AlexaFluoro-594 labeled siRNA (GeneDesign) were intravenously injected and US was exposed transdermally at 5 min after injection of BLs. At 1 h after injection, mice were sacrificed and liver was collected, rinsed with saline. Parenchymal cells (PCs) and NPCs were separated with collagenase perfusion and one-step density gradient centrifugation with 12.6% OptiPrep. Then, Kupffer cells were separated by magnetic cell sorting with phycoerythrin (PE)-labelled anti-mouse F4/80 antibody (Bay bioscience, Hyogo, Japan) and anti-PE antibody-conjugated microbeads (Miltenyi Biotec), and endothelial cells were separated by magnetic cell sorting with anti-mouse CD146 antibody (ME-9F1)-conjugated microbeads (Miltenyi Biotec) following the manufacturer's instructions. The isolated cells were suspended in lysis buffer (0.05% Triton X-100, 2 mM EDTA, 0.1 M Tris, pH 7.8), and then, the cell suspension was shaken, and centrifuged at $10,000 \times g$, 4 °C for 10 min. Fluorescence intensity derived from AlexaFluoro-594 was measured with FluoroMax-4 (Horiba) and the fluorescence intensity was normalized with respect to the number of cells.

For visualizing the hepatic localization of siRNA, liver were processed by the method of frozen section, and cut into 5 μ m thick sections with the use of cryostat (CM1850; Leica Microsystems, Wetzlar, Germany). Then, the HECs in the liver were stained by sheep anti-mouse CD146 antibody (R&D systems, Minneapolis, MN, USA) at 1:50 (v/v) dilution in PBS containing 5% FBS. As a second antibody, FITC-conjugated rabbit anti-sheep IgG antibody (MP Biomedicals, Irvine, CA) was used at 1:1000 (v/v) dilution in PBS containing 5% FBS. The sections were observed under the fluorescence microscope (Biozero BZ-8000; KEYENCE, Osaka, Japan), and the images obtained with different filters were afterwards overlaid.

Inflammatory stimulation by LPS, CCl₄, DMN, and IR. To induce LPS-stimulated inflammation *in vitro*, LPS (derived from Escherichia coli 0111:B4, 100 ng/mL; Sigma-Aldrich) was added to primary HECs at 24 h after siRNA transfer. LPS/D-galactosamine-induced hepatic inflammatory mouse model was prepared by intraperitoneal administration of LPS/D-galactosamine (1 μ g/100 mg/kg in saline) into mice at 24 h after siRNA delivery. To induce CCl₄- and DMN-stimulated hepatic inflammation, 2.0% CCl₄ (10 mL/kg in olive oil, Tokyo Chemical Industry, Tokyo, Japan) and 0.05% DMN (15 mL/kg in saline, Tokyo Chemical Industry) were administered intraperitoneally into mice

at 24 h after siRNA delivery, respectively. Moreover, hepatic IR-injury mouse model was prepared according to previously reported [8]. Briefly, an atraumatic clip was applied to interrupt the artery and portal venous blood supply to the left and middle liver lobes. After 60 min of partial hepatic warm ischemia, the clamp was removed to initiate hepatic reperfusion. This partial hepatic ischemia for 60 min results in a segmental hepatic ischemia (approximately 70%), and prevents mesenteric venous congestion by allowing portal decompression through the right lobes of the liver. Sham-operated mice were subjected to laparotomy and identical liver manipulations without vascular occlusion.

Measurement of the level of mRNA expression. At predetermined times following inflammatory stimulation, total RNA was collected from the cells and livers using a GenElute Mammalian Total RNA Miniprep Kit (Sigma-Aldrich, St. Louis, MO). Reverse transcription of mRNA was carried out using a PrimeScript RT reagent Kit (Takara Bio, Shiga, Japan). The detection of the ICAM-1 cDNA was carried out by real-time PCR using SYBR Premix Ex Taq (Takara Bio) and Lightcycler Quick System 350S (Roche Diagnostics, Indianapolis, IN) with primers. The primers for *icam-1* and *gapdh* cDNA were constructed as follows: primer for *icam-1* cDNA, 5'-TCG GTG GAT GGA GCA AGA-3' (forward) and 5'-CAG CAG GGG CAA TAG AGA ATG-3' (reverse); primer for *gapdh*, 5'-TCT CCT GCG ACT TCA ACA-3' (forward) and 5'-GCT GTA GCC GTA TTC ATT GT-3' (reverse) (Sigma-Aldrich). The mRNA copy numbers were calculated for each sample from the standard curve using the instrument software ('Arithmetic Fit Point analysis' for the Lightcycler). Results were expressed as relative copy numbers calculated relative to *gapdh* mRNA (copy numbers of *icam-1* mRNA/copy numbers of *gapdh* mRNA).

Evaluation of the level of protein expression on the cell membrane. At predetermined times following inflammatory stimulation, the mouse HECs were isolated and homogenized in PBS containing a cocktail of protease inhibitors (aprotinin; 2.0 µg/mL, leupeptin; 1.0 µg/mL, Pepstatin A; 1.0 µg/mL and PMSF; 100 µg/mL). The membranes of mouse HECs were isolated by density gradient centrifugation using OptiPrep. The protein concentration was determined with a Protein Quantification Kit (Dojindo Molecular Technologies). After incubated at 90 °C for 10 min, samples containing 20 µg of total protein were diluted with loading buffer and separated by SDS-PAGE using 10% polyacrylamide gel (SuperSep Ace;

Wako Pure Chemical Industries, Osaka, Japan). The separated protein bands were transferred to a polyvinylidene fluoride (PVDF) membrane (Hybond-P; GE Healthcare, Buckinghamshire, UK) by semidry blotting with Transblot SD (Bio-Rad, Hercules, CA). To avoid nonspecific binding, the membrane was incubated with Tris-buffered saline containing 3% bovine serum albumin (BSA). For the detection of ICAM-1 and GAPDH, goat anti-mouse ICAM-1 antibody and goat anti-mouse GAPDH antibody (Santa Cruz Biotechnology, Santa Cruz, CA, USA) were used at 1:100 (v/v) and 1:200 (v/v) dilution in Tris-buffered saline containing 1.0% BSA. As a second antibody, horseradish peroxidase (HRP)-conjugated rabbit anti-goat IgG antibody (R&D systems) was used at 1:10000 (v/v) dilutions in Tris-buffered saline containing 1% BSA. The protein band was detected with enhanced chemiluminescence (ECL) reagents (Millipore, Billerica, MA). Moreover, ICAM-1 levels on the membrane were also measured by the Opt-EIA Kit (BD Biosciences Pharmingen, San Diego, CA) according to the recommended procedures.

Immunohistochemical detection of ICAM-1. For visualizing ICAM-1, the cells fixed with 4% paraformaldehyde and the frozen liver sections were incubated with goat anti-mouse ICAM-1 antibody (Santa Cruz Biotechnology) used at 1:50 (v/v) dilution in PBS containing 5% FBS. Then, cells were followed by incubation with fluorescein isothiocyanate (FITC)-conjugated rabbit anti-goat IgG antibody (Santa Cruz Biotechnology) used at 1:400 (v/v) dilution in PBS containing 5% FBS. The cover glasses were mounted on slide glasses with VECTASHIELD mounting medium with DAPI (Vector Laboratories). The cells and the sections were observed using a Fluoview FV10i confocal laser microscope (Olympus) and a Biozero BZ-8000 fluorescence microscope (KEYENCE), respectively.

Measurement of inflammatory cytokines and aminotransferase activities in the serum. At predetermined times following inflammatory stimulation, serum were collected from the anesthetized mice. The cytokine levels (TNF- α , IFN- γ , and IL-6) in the serum were determined by the commercial ELISA Kit (Bay bioscience) according to the recommended procedures. Alanine aminotransferase (ALT) and aspartate aminotransferase (AST) activities in the serum were determined using Transaminase CII-Test Wako kit (Wako Pure Chemical Industries) according to manufacturer's instructions.

Detection of infiltrated leukocytes and apoptotic cells in the liver. For the detection of infiltrated leukocytes and apoptotic cells in the liver section, liver was excised from mice and processed by the method of frozen section cut into 5 μm thick sections with the use of cryostat (CM1850; Leica Microsystems). For visualizing infiltrated leukocytes, the frozen liver sections were incubated with rat anti-mouse Gr-1 (Ly-6G) antibody (R&D systems) used at 1:100 (v/v) dilution in PBS containing 5% FBS. Then, the sections were followed by incubation with rhodamine isothiocyanate (RITC)-conjugated goat anti-rat IgG antibody (Invitrogen) used at 1:400 (v/v) dilution in PBS containing 5% FBS. For visualizing apoptotic cells, TUNEL staining was performed by using in situ Apoptosis Detection Kit (Takara Bio) according to the recommended procedures of the kit. In brief, the liver sections were reacted with fluorescein isothiocyanate (FITC)-conjugated TdT enzyme for 1 h at 37°C. After washing twice with PBS, cover glasses were mounted on slide glasses with VECTASHIELD mounting medium with DAPI (Vector Laboratories). The sections were observed under the fluorescence microscope (Biozero BZ-8000).

Liver Histology. At 24 h following inflammatory stimulation, livers were excised and immediately fixed with 10% neutral buffered formalin for 24 h. Then, tissue samples were processed by the method of paraffin-embedded section cut into 5 μm sections. After removal of the paraffin with xylene and rehydration in graded alcohol, the sections were stained with hematoxylin/eosin. The histology of the liver sections was examined under a microscope (Biozero BZ-8000 fluorescence microscope).

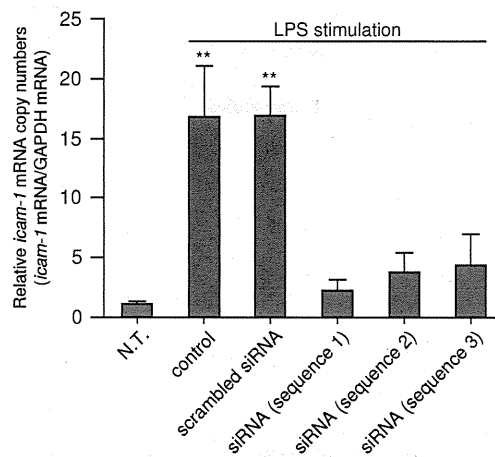
Supplementary Figure

Supplementary Fig. 1.

(A)

sequence 1	sense: GAAAGAU CAGGAUUAACAAdTdT antisense: UUGUAUAUCCUGAUCUUUCdTdT
sequence 2	sense: CAGAGAAAGAU CAGGAUUAUdTdT antisense: AUAUCCUGAUCUUUCUCUGdTdT
sequence 3	sense: GUACUGUACCACUCUCAAAAdTdT antisense: UUUGAGAGUGGUACAGUACdTdT
scrambled	sense: AAAUUAAAUGCGGAACAGdTdT antisense: CUGUUCGCAUUUUAAUUUdTdT

(B)



Supplementary Fig. 1. Suppression effects of 3 types of ICAM-1 siRNA on ICAM-1 expression in LPS-stimulated primary mouse HECs. (A) siRNA sequences used in this study. (B) Optimization of ICAM-1 siRNA sequence for the suppression of ICAM-1 expression in LPS-stimulated primary mouse HECs. HECs were exposed to LPS (100 ng/mL) at 24 h after transfection using 3 types of ICAM-1 siRNA (sequence 1, 2, and 3) using Lipofectamine 2000. After LPS stimulation for 24 h, quantitative RT-PCR were performed to analyze the expression level of *icam-1* and *gapdh* mRNA in LPS-stimulated primary mouse HECs. Each value represents the mean+SD (n=5). ** $P < 0.01$, compared with N.T.. N.T., no treatment.

Supplementary Fig. 2.

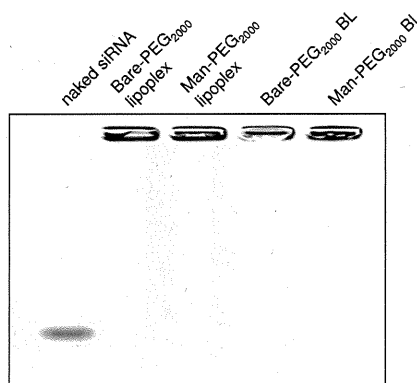
(A)

Particle sizes and ζ -potentials of liposomes and lipoplexes constructed with ICAM-1 siRNA with or without US imaging gas

	Particle size (nm)	ζ -potential (mV)
Bare-PEG ₂₀₀₀ liposome (DSTAP:DSPC:NH ₂ -PEG ₂₀₀₀ :DSPE=7:2:1 (mol))	102±4.3	60.2±6.8
Man-PEG ₂₀₀₀ liposome (DSTAP:DSPC:Man-PEG ₂₀₀₀ :DSPE=7:2:1 (mol))	107±5.1	63.7±4.7
Bare-PEG ₂₀₀₀ bubble liposome (DSTAP:DSPC:NH ₂ -PEG ₂₀₀₀ :DSPE=7:2:1 (mol))	551±30	62.9±6.9
Man-PEG ₂₀₀₀ bubble liposome (DSTAP:DSPC:Man-PEG ₂₀₀₀ :DSPE=7:2:1 (mol))	559±24	61.3±5.8
Bare-PEG ₂₀₀₀ lipoplex (DSTAP:DSPC:NH ₂ -PEG ₂₀₀₀ :DSPE=7:2:1 (mol))	106±5.9	47.2±4.2
Man-PEG ₂₀₀₀ lipoplex (DSTAP:DSPC:Man-PEG ₂₀₀₀ :DSPE=7:2:1 (mol))	108±6.2	49.7±6.2
Bare-PEG ₂₀₀₀ bubble lipoplex (BL) (DSTAP:DSPC:NH ₂ -PEG ₂₀₀₀ :DSPE=7:2:1 (mol))	568±49	49.8±7.8
Man-PEG ₂₀₀₀ bubble lipoplex (BL) (DSTAP:DSPC:Man-PEG ₂₀₀₀ :DSPE=7:2:1 (mol))	545±35	47.0±3.8

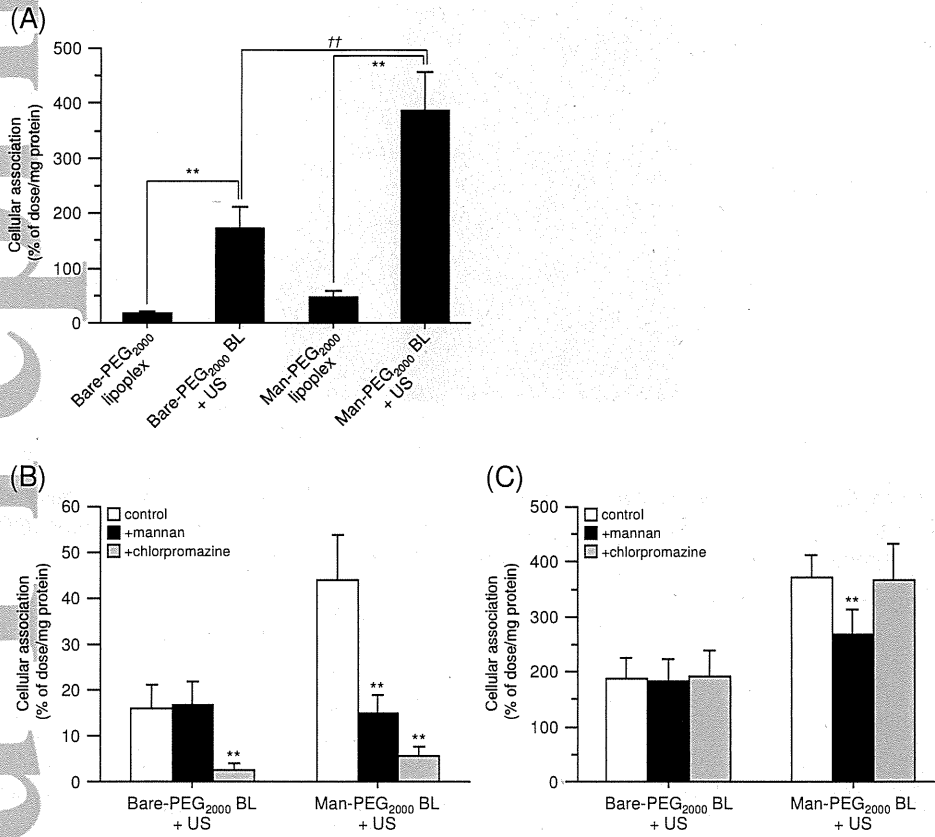
Each value represents the mean ± S.D. (n = 3).

(B)



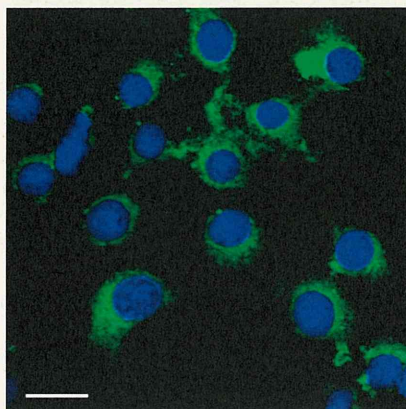
Supplementary Fig. 2. Physicochemical properties of Man-PEG₂₀₀₀ bubble liposome/ICAM-1 siRNA complexes. (A) Particle sizes and ζ -potentials of liposomes and lipoplexes constructed with ICAM-1 siRNA with or without US imaging gas. Each value represents the mean±SD (n=4). (B) Confirmation of siRNA complex by gel-retardation assay. Lipoplexes and BLs were constructed with AlexaFluor-488 labeled ICAM-1 siRNA and run on a 1% agarose gel.

Supplementary Fig. 3.



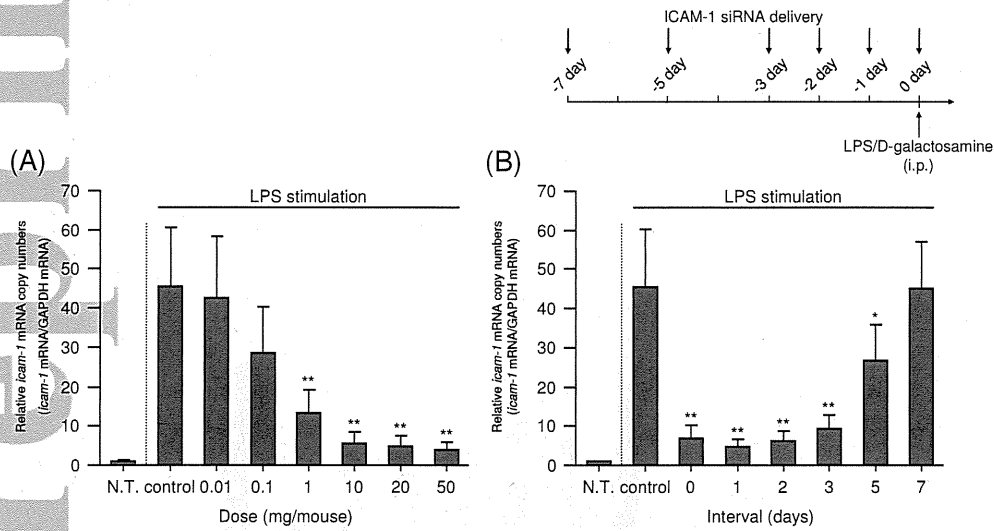
Supplementary Fig. 3. Enhancement of cellular associated siRNA by Man-PEG₂₀₀₀ BLs and US exposure *in vitro*. (A) Cellular association of AlexaFluor-594 labeled siRNA by transfection using bare-PEG₂₀₀₀ lipoplexes, bare-PEG₂₀₀₀ BLs with US exposure, Man-PEG₂₀₀₀ lipoplexes and Man-PEG₂₀₀₀ BLs with US exposure (1 μ g siRNA) at 2 h after addition of each lipoplex. Each value represents the mean+SD (n=5). Significant difference; **, ^{††} $P < 0.01$. (B,C) Inhibition of cellular associated siRNA by bare-PEG₂₀₀₀ lipoplexes, Man-PEG₂₀₀₀ lipoplexes, bare-PEG₂₀₀₀ BLs with US exposure, and Man-PEG₂₀₀₀ BLs with US exposure (1 μ g siRNA) in the absence or presence of 1 mg/mL mannan and 50 μ M chlorpromazine at 2 h after addition of each lipoplex. Each value represents the mean+SD (n=5). ** $P < 0.01$, compared with the corresponding group of control.

Supplementary Fig. 4.



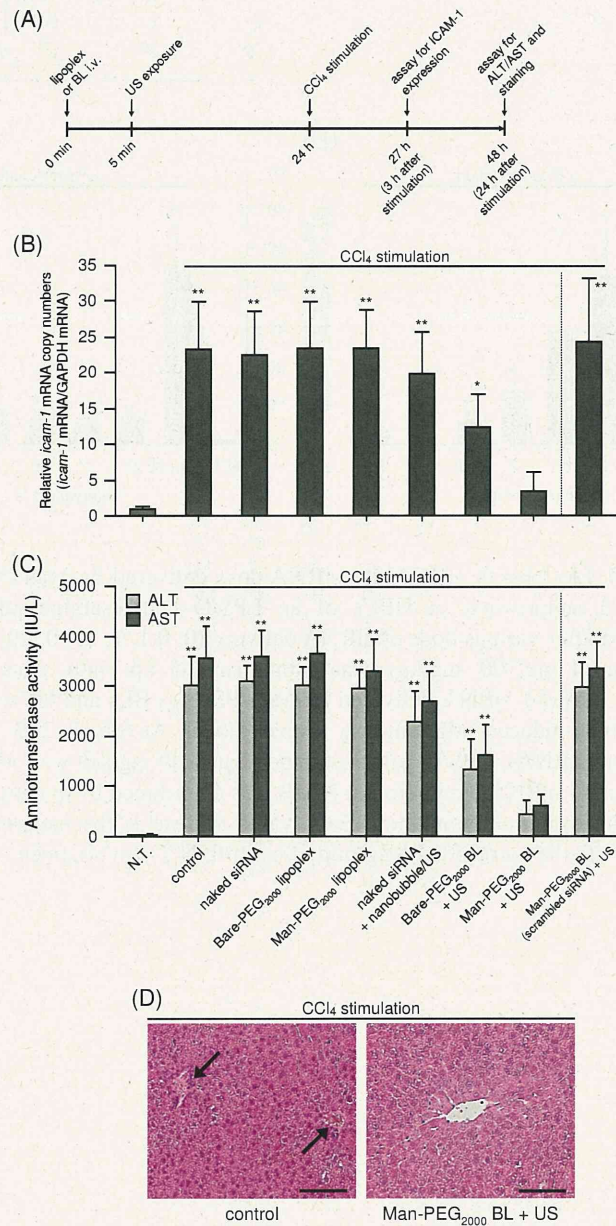
Supplementary Fig. 4. Confirmation of mannose receptor expression on primary mouse HECs. Primary mouse HECs were isolated from mice, and labeled with anti-mannose receptor (CD206) antibody (green). Nuclei were counterstained with DAPI (blue). Scale bar, 20 μ m.

Supplementary Fig. 5.



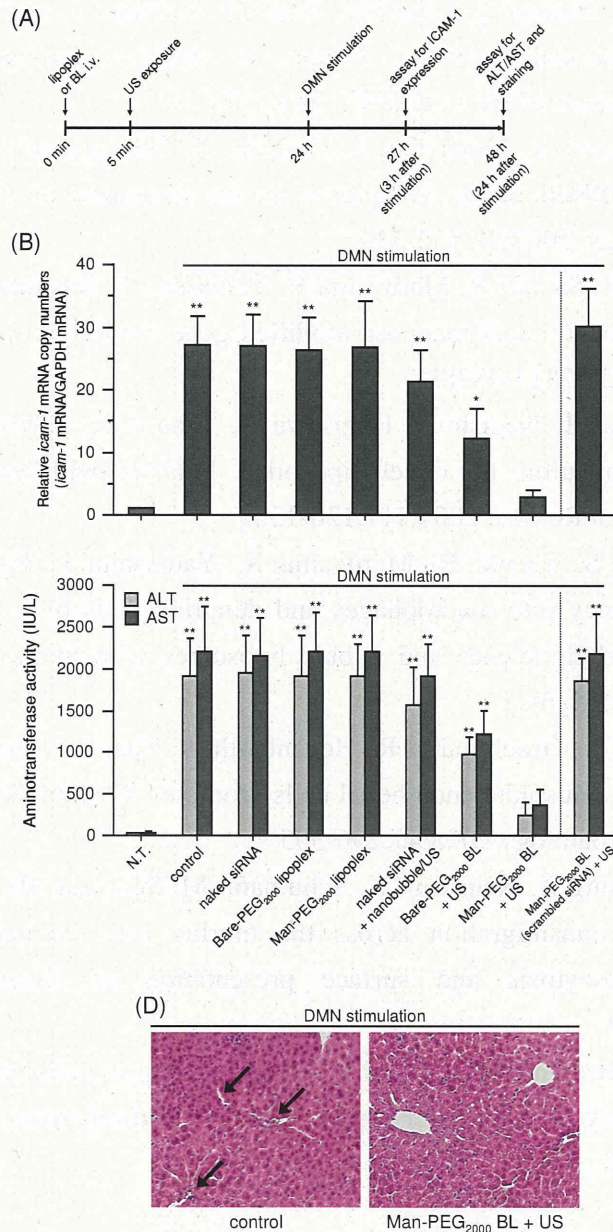
Supplementary Fig. 5. (A) Effects of ICAM-1 siRNA dose delivered by Man-PEG₂₀₀₀ BLs and US exposure on ICAM-1 suppression in HECs of an LPS/D-galactosamine-induced inflammatory mouse model. At 24 h after various dose of siRNA delivery (0, 0.1, 1, 3, 10, 20, and 50 μ g siRNA), LPS/D-galactosamine (1 μ g/100 mg/kg) was administrated i.p. into mice. (B) Duration of suppression effect of ICAM-1 siRNA delivered by Man-PEG₂₀₀₀ BLs and US exposure in HECs of an LPS/D-galactosamine-induced inflammatory mouse model. At 6 h, 1, 2, 3, 5, and 7 days after siRNA delivery (10 μ g siRNA), LPS/D-galactosamine (1 μ g/100 mg/kg) was administrated i.p. into mice. The level of *ICAM-1* mRNA expression in HECs was determined by quantitative RT-PCR at 3 h following LPS/D-galactosamine stimulation. Each value represents the mean+SD (n=5). * P <0.05; ** P <0.01, compared with the corresponding group of control. N.T., no treatment.

Supplementary Fig. 6.



Supplementary Fig. 6. Suppression effects of ICAM-1 siRNA delivery using Man-PEG₂₀₀₀ BLs and US exposure on *icam-1* mRNA expression and liver toxicity in an CCl₄-induced inflammatory mouse model. (A) Evaluation schedule using CCl₄-induced inflammatory mouse model. (B) The level of *icam-1* mRNA expression obtained by ICAM-1 siRNA delivery (10 μg siRNA) using various delivery methods in HECs. At 24 h after siRNA delivery, CCl₄ (2.0%; 10 mL/kg in olive oil) was administered i.p. into mice. *icam-1* mRNA expression in HECs was determined by quantitative RT-PCR at 3 h following CCl₄ stimulation. (C) The level of serum ALT/AST activities followed by siRNA delivery (10 μg siRNA) using various delivery methods at 24 h following CCl₄ stimulation. **P*<0.05; ***P*<0.01, compared with the corresponding group of N.T.. Each value represents the mean±SD (n=5). N.T., no treatment. (D) Photomicrographs of liver histology followed by siRNA delivery using Man-PEG₂₀₀₀ BLs (10 μg siRNA) and US exposure in CCl₄-induced inflammatory mouse model. Livers were embedded in paraffin, sectioned, and stained with H&E. Black arrows: destruction of tube formation in hepatic central vein. Scale bars, 100 μm.

Supplementary Fig. 7.



Supplementary Fig. 7. Suppression effects of ICAM-1 siRNA delivery using Man-PEG₂₀₀₀ BLs and US exposure on *icam-1* mRNA expression and liver toxicity in an DMN-induced inflammatory mouse model. (A) Evaluation schedule using DMN-induced inflammatory mouse model. (B) The level of *icam-1* mRNA expression obtained by ICAM-1 siRNA delivery (10 μ g siRNA) using various delivery methods in HECs. At 24 h after siRNA delivery, DMN (0.05%; 15 mL/kg in saline) was administered i.p. into mice. *icam-1* mRNA expression in HECs was determined by quantitative RT-PCR at 3 h following DMN stimulation. (C) The level of serum ALT/AST activities followed by siRNA delivery (10 μ g siRNA) using various delivery methods at 24 h following DMN stimulation. * P <0.05; ** P <0.01, compared with the corresponding group of N.T.. Each value represents the mean+SD (n =5). N.T., no treatment. (D) Photomicrographs of liver histology followed by siRNA delivery using Man-PEG₂₀₀₀ BLs (10 μ g siRNA) and US exposure in DMN-induced inflammatory mouse model. Livers were embedded in paraffin, sectioned, and stained with H&E. Black arrows: destruction of tube formation in hepatic central vein. Scale bars, 100 μ m.

Supplementary References

1. Tai ES, bin Alib A, Zhangb Q, Loha LM, Tana CE, Retnamc L, et al. Hepatic expression of PPAR α , a molecular target of fibrates, is regulated during inflammation in a gender-specific manner. *FEBS Lett.* 2003, 546:237-240.
2. Higuchi Y, Kawakami S, Yamashita F, Hashida M. The potential role of fucosylated cationic liposome/NF κ B decoy complexes in the treatment of cytokine-related liver disease. *Biomaterials.* 2007;28:532-539.
3. Un K, Kawakami S, Suzuki R, Maruyama K, Yamashita F, Hashida M. Development of an ultrasound-responsive and mannose-modified gene carrier for DNA vaccine therapy. *Biomaterials* 2010;31:7813-7826.
4. Suzuki R, Takizawa T, Negishi Y, Hagsawa K, Tanaka K, Sawamura K, et al. Gene delivery by combination of novel liposomal bubbles with perfluoropropane and ultrasound. *J Control Release* 2007;117:130-136.
5. Un K, Kawakami S, Suzuki R, Maruyama K, Yamashita F, Hashida M. Enhanced transfection efficiency into macrophages and dendritic cells by a combination method using mannosylated lipoplexes and bubble liposomes with ultrasound exposure. *Hum Gene Ther* 2010;21:65-74.
6. Diehl L, Schurich A, Grochtmann R, Hegenbarth S, Chen L, Knolle PA. Tolerogenic maturation of liver sinusoidal endothelial cells promotes B7-homolog 1-dependent CD8+ T cell tolerance. *Hepatology* 2008;47:296-305.
7. Schrage A, Wechsung K, Neumann K, Schumann M, Schulzke JD, Engelhardt B, et al. Enhanced T cell transmigration across the murine liver sinusoidal endothelium is mediated by transcytosis and surface presentation of chemokines. *Hepatology* 2008;48:1262-1272.
8. Park SW, Kim M, Brown KM, D'Agati VD, Lee HT. Paneth cell-derived interleukin-17A causes multiorgan dysfunction after hepatic ischemia and reperfusion injury. *Hepatology* 2011;53:1662-1675.